Cell Metabolism, Volume *29*

Supplemental Information

Mitochondrial DNA Variation Dictates Expressivity and Progression of Nuclear DNA Mutations Causing Cardiomyopathy

Meagan J. McManus, Martin Picard, Hsiao-Wen Chen, Hans J. De Haas, Prasanth Potluri, Jeremy Leipzig, Atif Towheed, Alessia Angelin, Partho Sengupta, Ryan M. Morrow, Brett A. Kauffman, Marc Vermulst, Jagat Narula, and Douglas C. Wallace

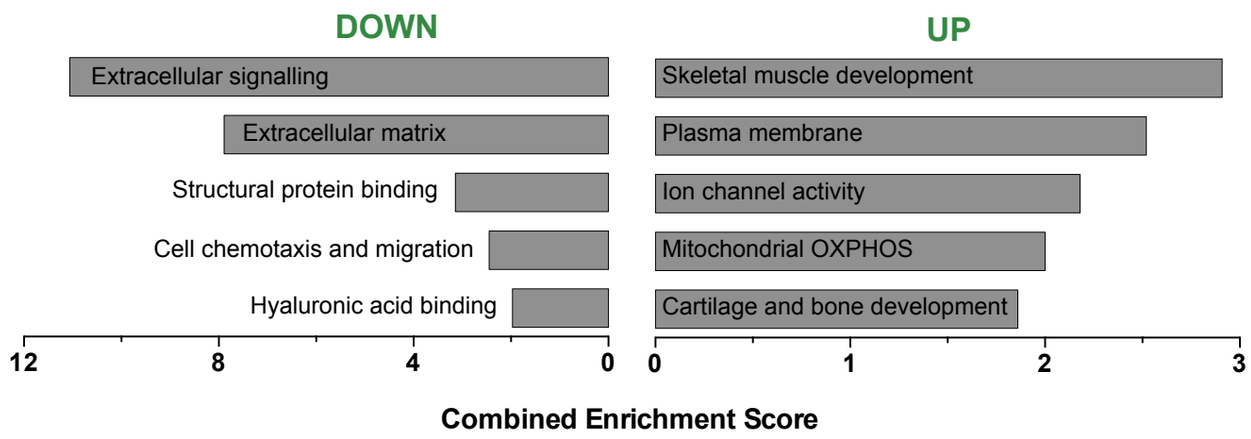

Figure S1. Related to Figure 1: Integrative analysis by clustering of functional annotation terms. Functional cluster analysis revealed significant repression of pathways associated with extracellular matrix maintenance and signaling, structural protein binding, and cell chemotaxis and migration signaling, which together contribute to organ pattern formation. The overexpression of contractile and fibrous components specific to skeletal muscle, cartilage and bone development also mark the loss of myocardial integrity and increased fibrosis observed in cardiac remodeling of the *Ant1*-null heart.

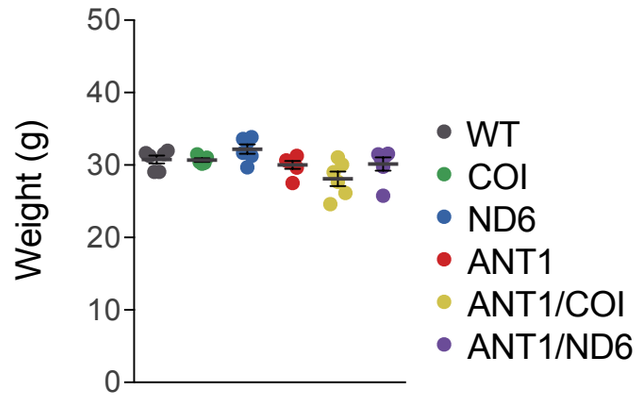

Figure S2. Related to Figure 2: Average body weight per strain. Body weights are indistinguishable between strains of age-matched mice that underwent indirect calorimetry screening at 6 mo. ($p \geq 0.56$).

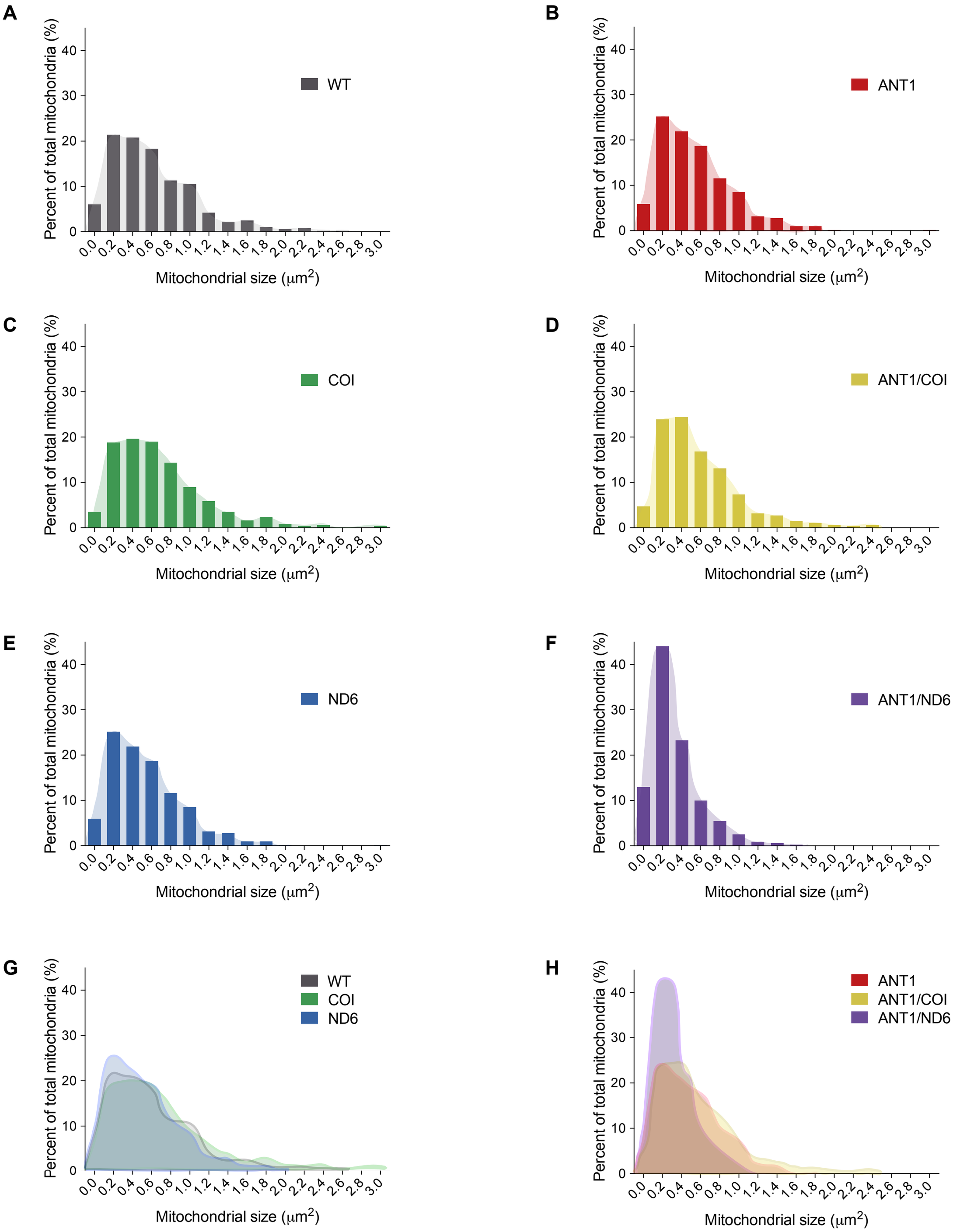

Figure S3. Related to Figure 4: Effect of mitochondrial mutations on mitochondrial size distribution. (**A-H**) Histograms reveal the diametrically opposed influence of mtDNA *COI*^{V421A} and *ND6*^{P25L} variants on (**A**) WT mitochondrial size. (**C**) *COI*^{V421A} increases mitochondrial size up to 3.0 um$_2$, and brings (**B**) *Ant*$^{-/-}$ mitochondria back within WT range (0 - 2.4 um^2; **D,** ANT1/COI). (**E**) *ND6*^{P25L} causes mitochondrial fragmentation, and acts synergistically with nDNA *Ant*$^{-/-}$, *r*educing most mitochondria to 0.2 um^2 (**F,** ANT1/ND6**)**. (**G-H**) Overlay of each mtDNA genotype on the nDNA (**G**) WT or (**H**) *Ant*$^{-/-}$ background.

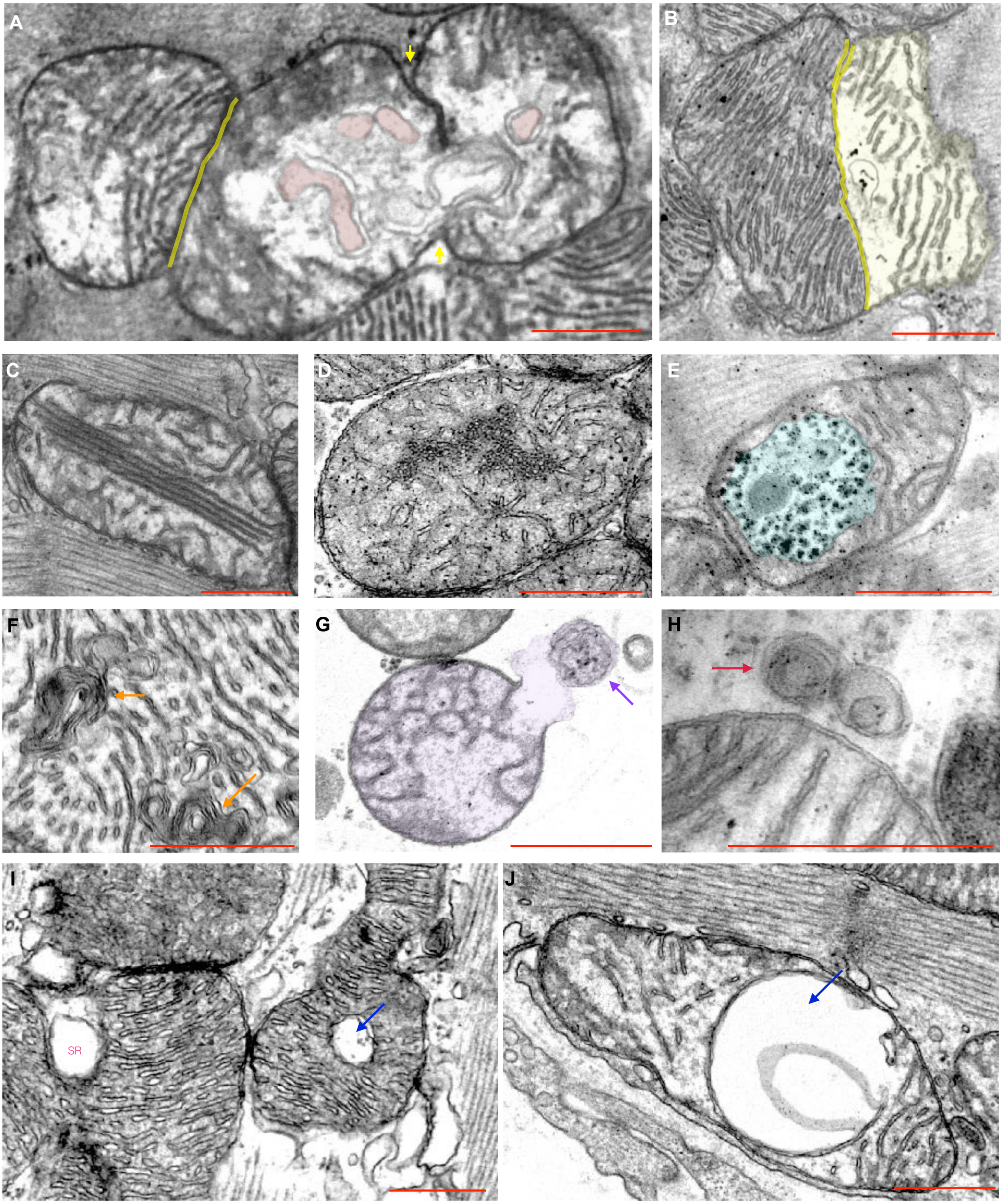

Figure S4. Related to Figure 4: Intramitochondrial abnormalities caused by loss of ANT1. (**A-B**) Fission-associated partitioning cristae (yellow tracings) divide defective, hypodense regions (yellow shading, **B**) with circular cristae (red shading, **A**). (**B**) Yellow arrows highlight fission-associated pinching of the OMM. (**C-E**) Intramitochondrial inclusions formed by (**C**) paracrystalline cristae or (**D**) aggregates of malformed cristae, or (**E**) compartmentalized by an inner membrane boundary. (**F**) Dense packing of circular cristae into concentric inclusions (orange arrows). (**G**) Mitochondrial release of concentric membrane components (purple arrow) into the cytoplasm, possibly for degradation or signaling as mitochondrial-derived vesicles (**H**; red arrow, (Cadete et al., 2016). (**I-J**) Membrane-bound hypodense regions (blue arrows), which may represent mitochondrial spheroids (**I;** (Ding et al., 2012) or cristolysis (**J**). Scale bars (red) = 500nm.

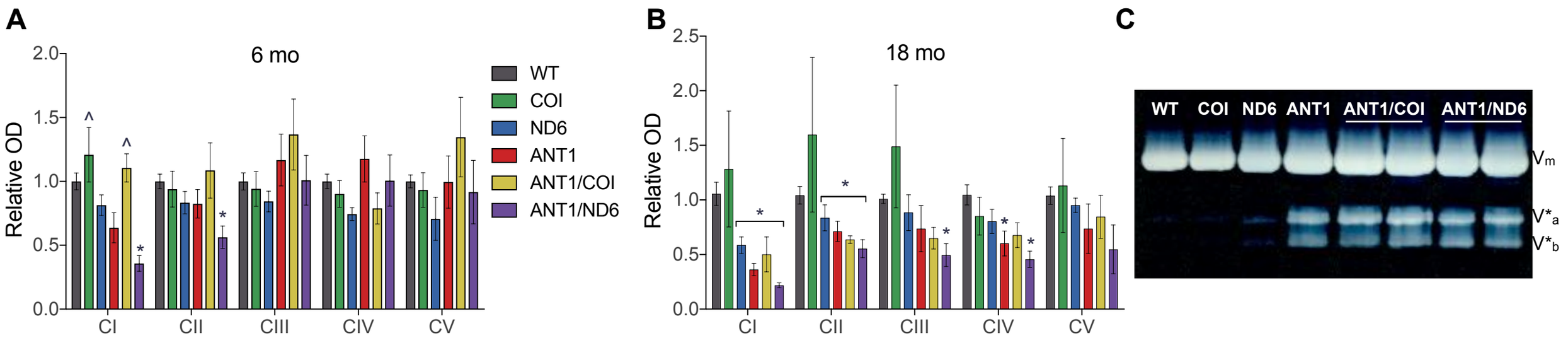

Figure S5. Related to Figure 5: Effect of nDNA-mtDNA on specific subunits of OXPHOS I-V and F_1F_o-ATPase structural assembly. (**A-B**) Densitometric analysis of OXPHOS CI subunit NDUFB8, CII subunit SDHB, CIII subunit UQCRC2, CIV subunit COI, and CV ATP5A from heart mitochondria isolated from mice at (**A**) 6 and (**B**) 18 mo. of age, normalized to the age-matched WT control (*$p < 0.05$ vs. WT; ^$p < 0.01$ vs ANT1; n = 4 - 7). (**C**) Clear native electrophoresis (CNE) of maltoside-solubilized (2.5% w/v) heart mitochondria (50 µg) showing loss of ANT1 destabilizes the F_1F_o-ATPase holo-complex (V_m) by the appearance of lower molecular weight subcomplexes (V*a, V*b) (n = 3).

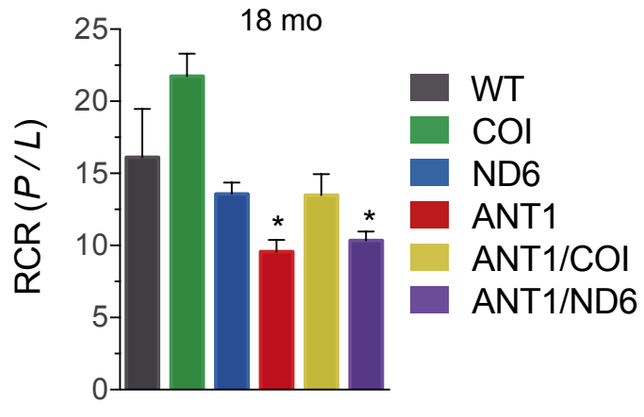

Figure S6. Related to Figure 6: mtDNA *CO*I^{N421A} prevents the decline in mitochondrial function due to loss of *Ant1*$^{-/-}$ in the aged heart. The respiratory control ratio (RCR) is shown as the ratio of ADP-stimulated to LEAK (P:L) states from cardiac mitochondria isolated from mice at 18mo. of age (*$p < 0.05$ vs. WT; n = 3 – 5).

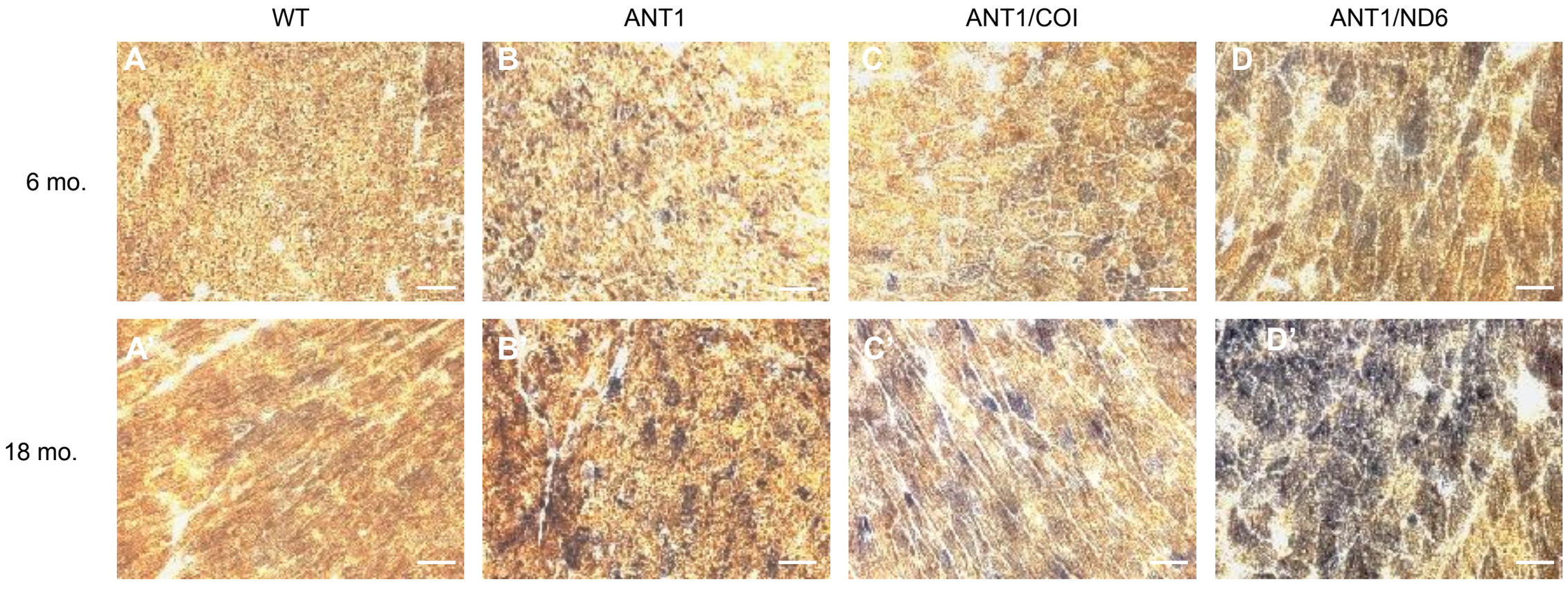

Figure S7. Related to Figure 7: COX and SDH histochemistry in aged myocardium. (A-D') Representative images of combined histochemical reactions for mitochondrial enzymes COX (brown) and SDH (blue) in the myocardium of mice from the following strains at 6 and 18 mo. of age, respectively: WT (A, A'), ANT1 (B, B'), ANT1/COI (C, C'), and ANT1/ND6 (D, D'). COX-deficient cardiac myocytes (blue) increase with age and are most prolific in mtDNA-nDNA combination strains with the highest mtDNA deletion load (original magnification × 20). Scale bar = 50 uM.

Table S1. Related to Figure 1.

nDNA Gene	Fold Δ	p adj	mtDNA Gene	Fold Δ	p adj
Ndufa1	**0.66**	0.73	mt-Nd1	**2.07**	0.08
Ndufa10	**0.96**	1.00	mt-Nd2	**3.27**	0.00
Ndufa11	**0.91**	0.98	mt-Nd3	**8.03**	0.00
Ndufa12	**0.97**	1.00	mt-Nd4	**2.14**	0.04
Ndufa13	**0.74**	0.88	mt-Nd5	**2.50**	0.13
Ndufa2	**1.14**	0.94	mt-Nd6	**3.74**	0.00
Ndufa3	**0.66**	0.70	mt-Cytb	**1.94**	0.15
Ndufa5	**0.87**	0.97	mt-Co1	**1.56**	0.76
Ndufa6	**0.90**	0.97	mt-Co3	**2.04**	0.37
Ndufa7	**0.78**	0.88	mt-Ta	**2.16**	0.72
Ndufa8	**0.89**	0.97	mt-Tc	**0.94**	0.97
Ndufa9	**0.86**	0.94	mt-Tf	**5.12**	0.01
Ndufab1	**0.75**	0.81	mt-Ti	**2.16**	0.65
Ndufb10	**0.84**	0.95	mt-Tl1	**2.28**	0.12
Ndufb11	**0.74**	0.84	mt-Tl2	**0.91**	0.95
Ndufb2	**2.76**	0.00	mt-Tm	**1.50**	0.81
Ndufb3	**0.74**	0.84	mt-Tp	**1.45**	0.93
Ndufb4	**0.80**	0.87	mt-Tq	**2.08**	0.78
Ndufb5	**0.77**	0.86	mt-Tr	**1.10**	1.00
Ndufb6	**0.84**	0.92	mt-Ts2	**0.99**	0.98
Ndufb7	**0.90**	0.98	mt-Tt	**2.63**	0.05
Ndufb8	**0.94**	0.99	mt-Tv	**1.39**	0.91
Ndufb9	**0.89**	0.98	mt-Rnr1	**2.26**	0.15
Ndufc1	**0.62**	0.47	mt-Rnr2	**0.81**	0.96
Ndufc2	**0.80**	0.87			
Ndufs1	**0.75**	0.83			
Ndufs2	**0.78**	0.89			
Ndufs3	**1.02**	1.00			
Ndufs4	**0.84**	0.92			
Ndufs5	**0.73**	0.81			
Ndufs6	**0.69**	0.77			
Ndufs7	**0.81**	0.92			
Ndufs8	**1.01**	1.00			
Ndufv1	**0.74**	0.86			
Ndufv2	**0.82**	0.90			
Ndufv3	**0.94**	1.00			
Sdha	**0.78**	0.89			
Sdhb	**0.77**	0.88			
Sdhc	**0.71**	0.81			
Sdhd	**1.05**	0.98			
Cyc1	**0.85**	0.95			
Uqcr10	**0.73**	0.83			
Uqcr11	**0.75**	0.92			
Uqcrb	**0.72**	0.82			
Uqcrc1	**0.88**	0.96			

Table S1. Related to Figure 1.

nDNA Gene	Fold Δ	p adj
Uqcrc2	**1.25**	0.88
Uqcrfs1	**0.84**	0.94
Uqcrh	**1.13**	0.95
Uqcrq	**0.73**	0.83
Cox4i1	**0.80**	0.94
Cox4i2	**1.11**	0.96
Cox5a	**0.91**	0.99
Cox5b	**0.97**	0.99
Cox6a1	**0.85**	0.95
Cox6a2	**0.84**	0.95
Cox6b1	**0.71**	0.79
Cox6c	**0.83**	0.94
Cox7a1	**0.66**	0.77
Cox7a2	**0.58**	0.41
Cox7b	**0.78**	0.90
Cox7c	**0.65**	0.84
Cox8a	**0.80**	0.89
Atp5a1	**0.87**	0.96
Atp5b	**0.74**	0.88
Atp5c1	**1.02**	0.99
Atp5d	**0.95**	1.00
Atp5e	**0.71**	0.81
Atp5f1	**0.87**	0.95
Atp5g1	**1.08**	0.97
Atp5g3	**1.02**	1.00
Atp5h	**0.89**	0.97
Atp5j	**0.73**	0.83
Atp5j2	**0.83**	0.94
Atp5l	**0.92**	1.00
Atp5o	**0.77**	0.85
Atpif1	**1.08**	0.97

Table S1. Related to Figure 1. OXPHOS mRNA transcripts. Total mtRNA and nRNA-OXPHOS transcripts detected by RNASeq analysis from the left ventricle, shown as fold change (bold) of ANT1 from WT age-matched control, and the adjusted p value.

Table S2. Related to Figure 3.

ECG	WT		COI		ND6		ANT1		COI ANT1		ND6 ANT1	
Measure	Mean	S.D.	Mean	S.D.	Mean	S.D.	Mean	S.D.	Mean	S.D.	Mean	S.D.
SepTd	0.73	0.09	0.74	0.13	0.77	0.11	0.97*	0.12	0.95*	0.13	0.86	0.13
LVEDD	4.25	0.33	4.33	0.25	4.25	0.32	5.22*	0.44	5.51*	1.10	6.62*◆	0.95
PWTd	0.75	0.10	0.79	0.11	0.81	0.12	1.02*	0.14	0.91*	0.13	0.86*◆	0.14
SepTs	1.05	0.13	1.10	0.20	1.05	0.17	1.20*	0.12	1.16*	0.16	1.02	0.15
LVSED	3.07	0.30	3.05	0.25	3.03	0.38	4.30*	0.53	4.67	1.34	6.17*◆	0.98
PWTs	1.07	0.16	1.13	0.17	1.13	0.11	1.29*	0.25	1.09◆	0.22	1.03◆	0.13
FS	27.64	3.24	29.54	3.71	28.79	4.46	17.87*	5.20	16.19*	9.27	7.07*◆	3.18
EF	61.90	5.06	64.74	5.29	63.49	6.51	43.98*	10.23	39.15	18.41	19.49*◆	8.26
LV mass	116.91	22.87	128.20	29.85	127.98	27.49	245.10*	47.11	248.14*	74.84	305.80*◆	70.77
RWT	0.35	0.05	0.37	0.05	0.38	0.07	0.39	0.06	0.34	0.07	0.27*◆	0.06
Global Strain:												
Longitud-inal	-13.66	3.70	-13.62	3.06	-11.59	4.53	-7.68*	3.99	-8.87*	4.67	-2.64*◆	1.77
Circumfer-enctial	-18.33	4.64	-19.38	3.51	-17.44	3.17	-11.25*	3.85	-13.04*	7.89	-4.72*◆	2.12
Radial	23.81	6.93	26.05	8.08	23.98	5.82	17.52*	6.56	17.78*	8.24	8.20*◆	3.30

Table 2. Related to Figure 3. Echocardiographic parameters. Data are expressed as mean ± standard deviation (S. D.); *p ≤ 0.03 *vs*. WT; ◆p ≤ 0.03 *vs*. ANT1. Abbreviations: SepTd, septal thickness at diastole; LVDD, left ventricular diastolic diameter; PWTd, Posterior wall thickness diastole; SepTs, septal thickness at systole; LVSD left ventricular systolic diameter; FS, fractional shortening; EF, ejection fraction; LV, left ventricle; RWT, relative wall thickness.